Project Title: Intraseasonal Variability of the Monsoon Systems of the Americas: Processes, predictability and prediction

PI Names:Peter J. Webster

E-mail: pjw@eas.gatech.edu

Report Year: 2

Figures:

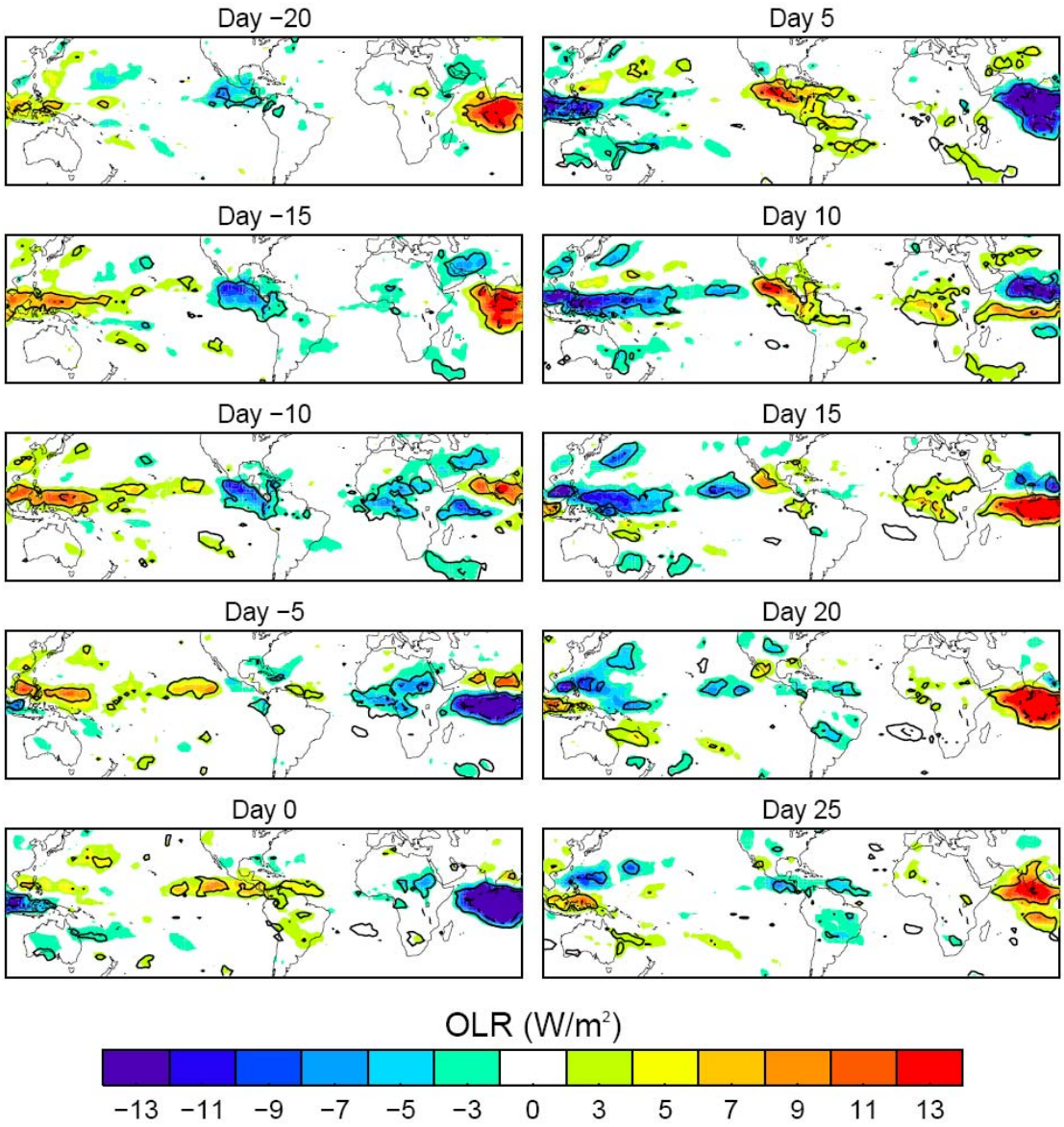

Figure 1. Composites of OLR for the Summer MJO

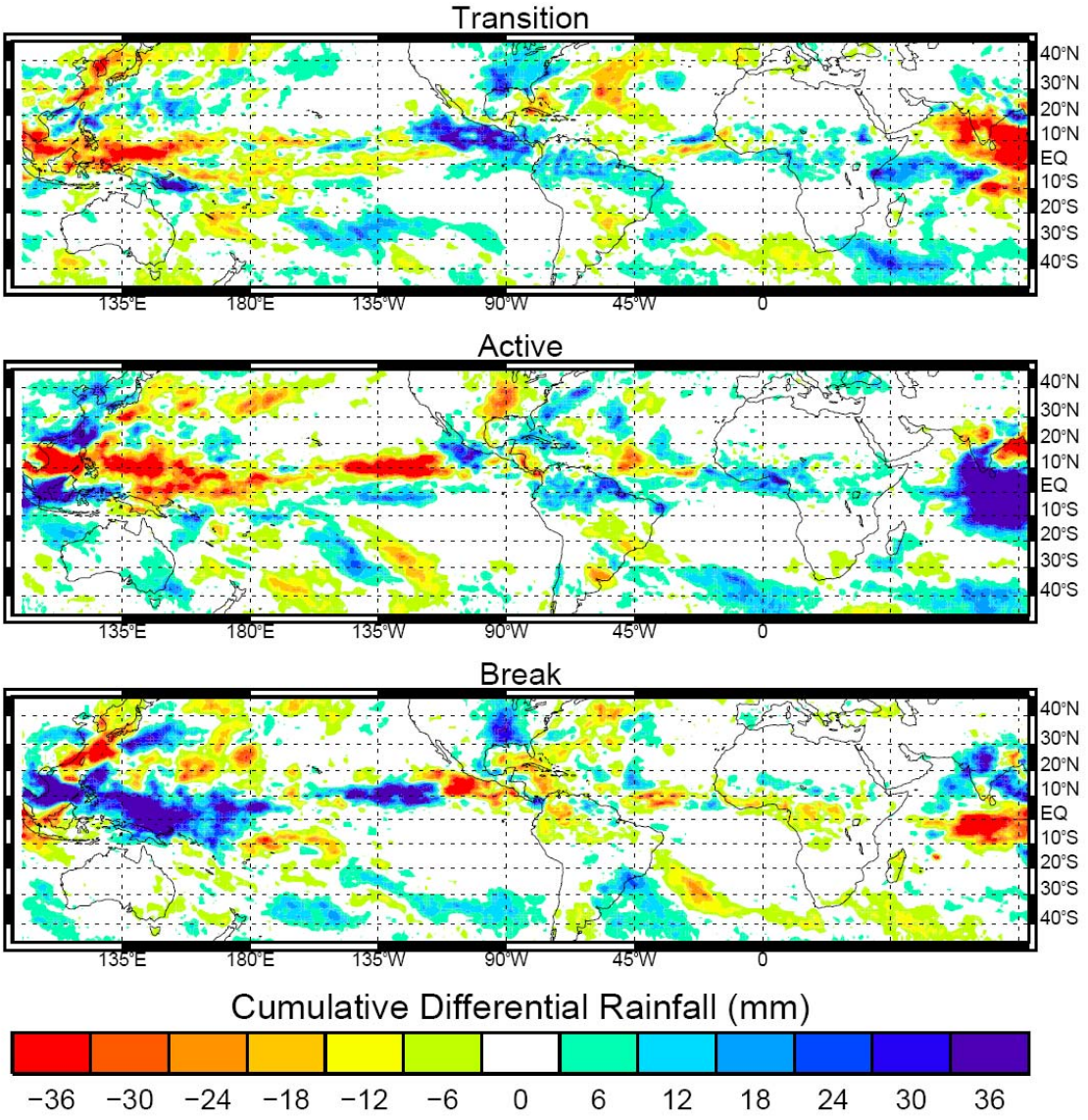

Figure 2. Difference of cumulative rainfall between two different phases of the summer MJO.

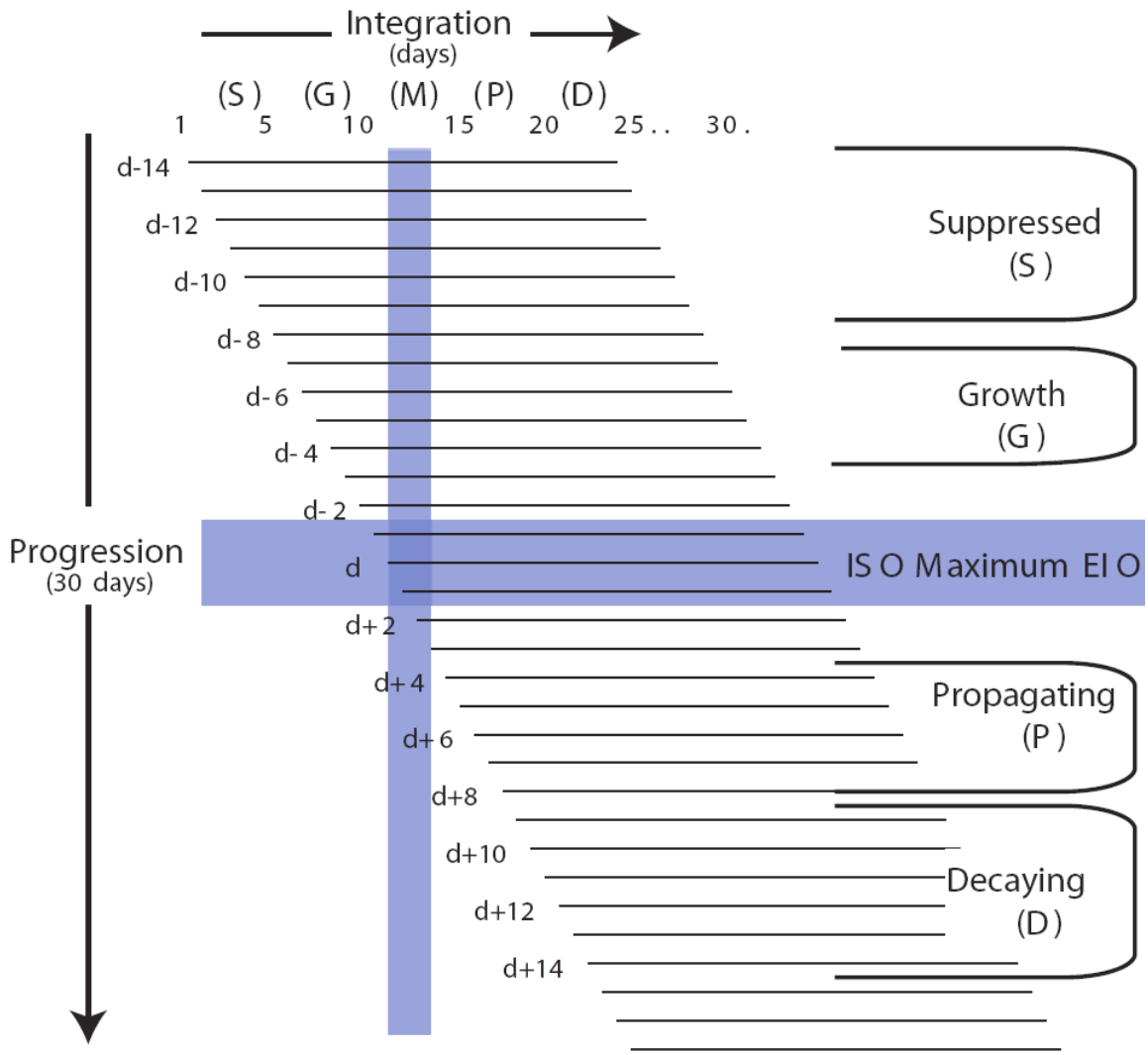

Figure 3. Schematic diagram of the extended serial integrations. Blue regions show the timing of the maximum amplitude of the ISO (M) in a specified region between the suppressed (S), growth (G), propagating (P) and decaying (D) phases of the event.

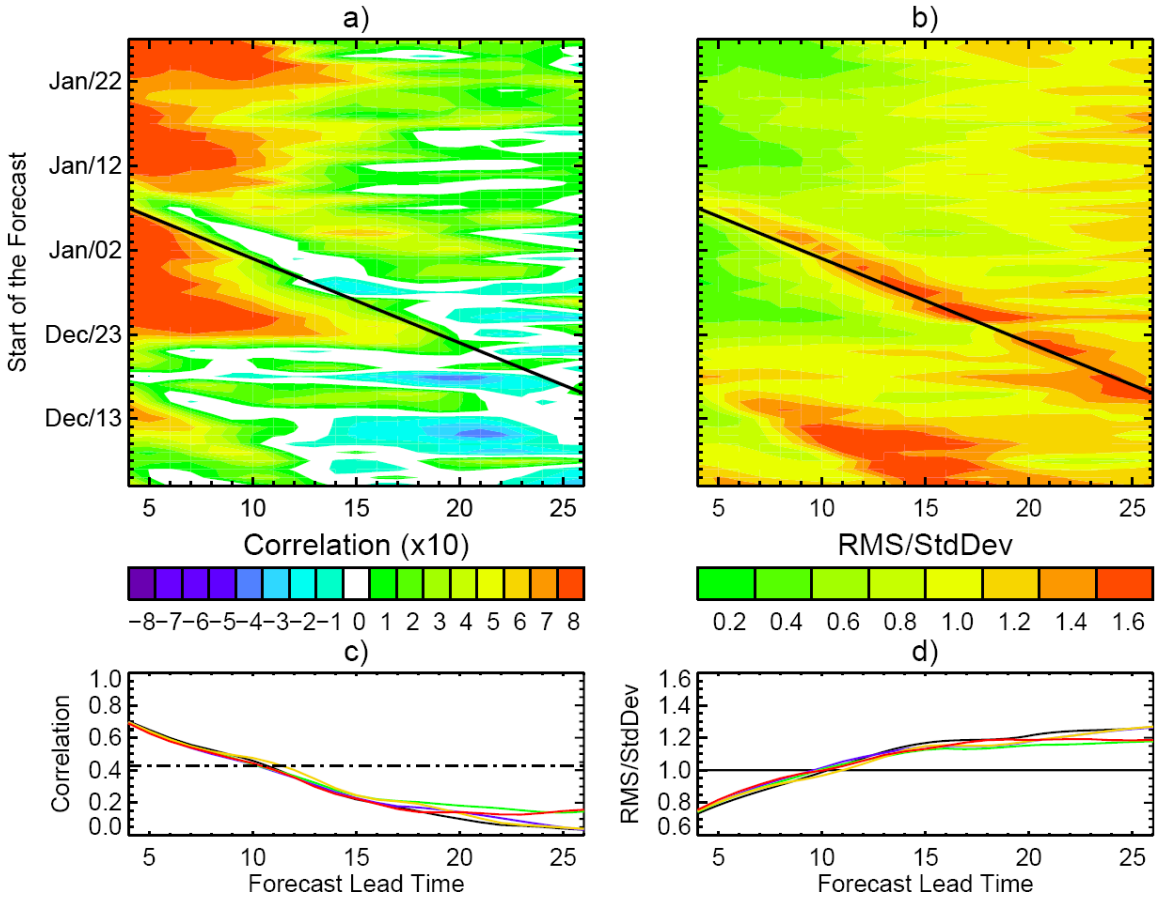

Figure 4. Distribution of the a) correlation and b) standardized RMS for the control run as a function of forecast lead time and start of the forecast for vertical anomalies of zonal winds in the Indo-West Pacific region (10°S-10N 60°E-170°W). Average c) correlation and d) RMS error estimated from the vertical structure of the anomalies from 1000 to 200 hPa for the control run (black line) and all ensemble members (color lines). Dash-dotted line corresponds to the 99% statistical significance threshold. Significance was estimated using Student's t-test.

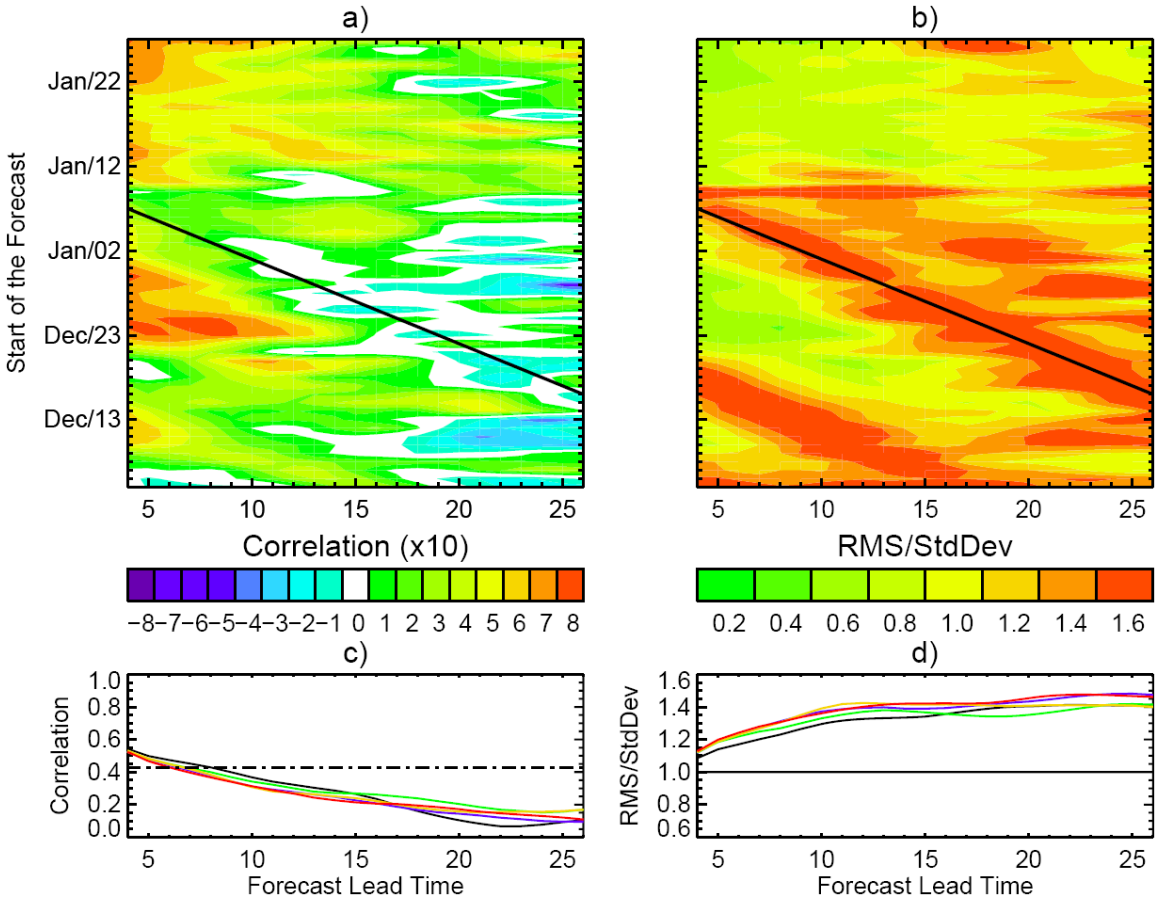

Figure 5. Same as Figure 1 but for specific humidity.

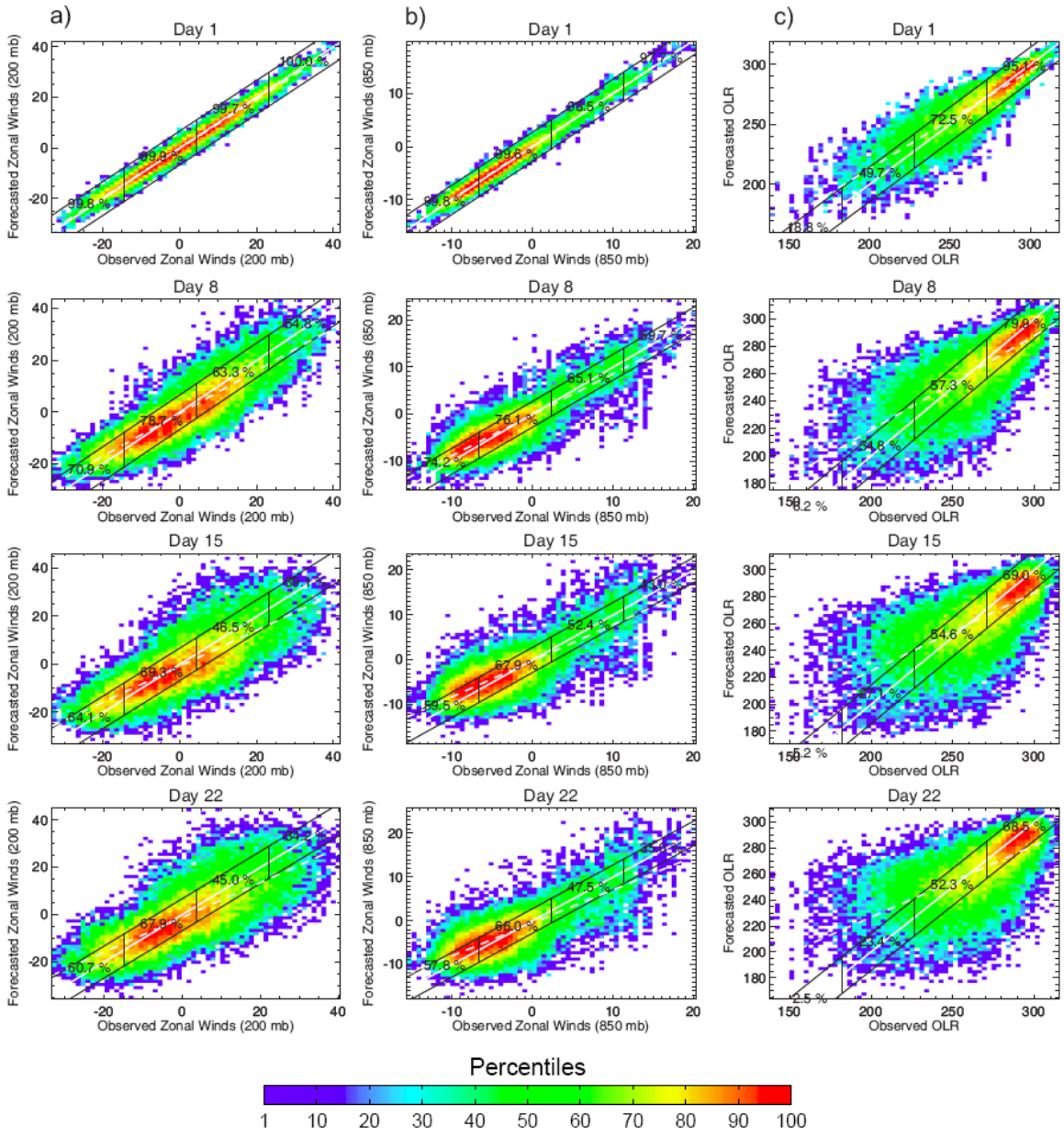

Figure 6. Joint probability density function between observed and forecasted a) 200 hPa and b) 850 hPa zonal winds (ms^{-1}) and c) OLR (Wm^{-2}) for different lead times (1, 8, 15 and 22) over the entire equatorial region (20°S-20°N 0°-360°E). The probability density increases from blue to red. The white continuous line corresponds to perfect forecasting and the dashed line to the actual linear fit between forecasts and observations. The black lines correspond to half standard deviation of the observations.

a) EOFs of OLR

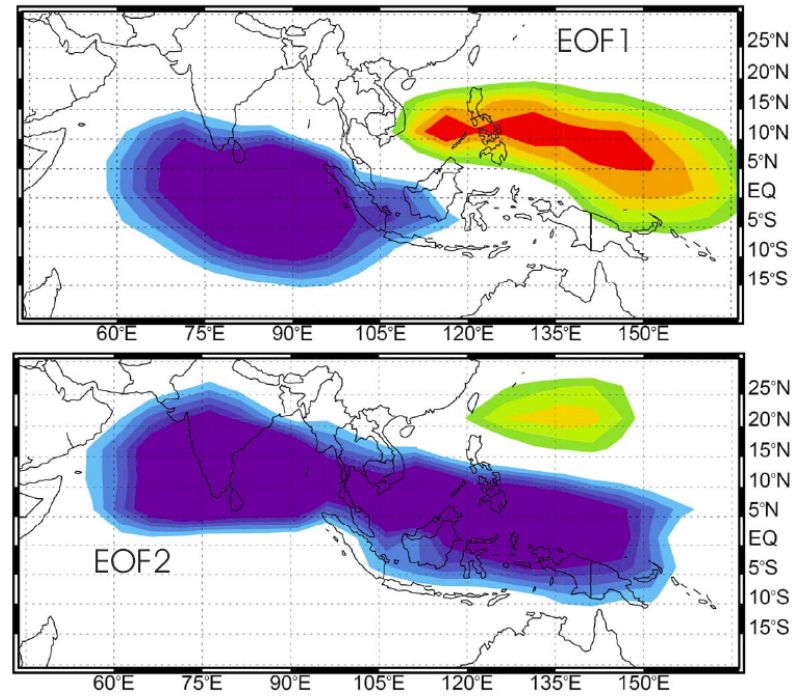

b) Fourier Spectra of PCs

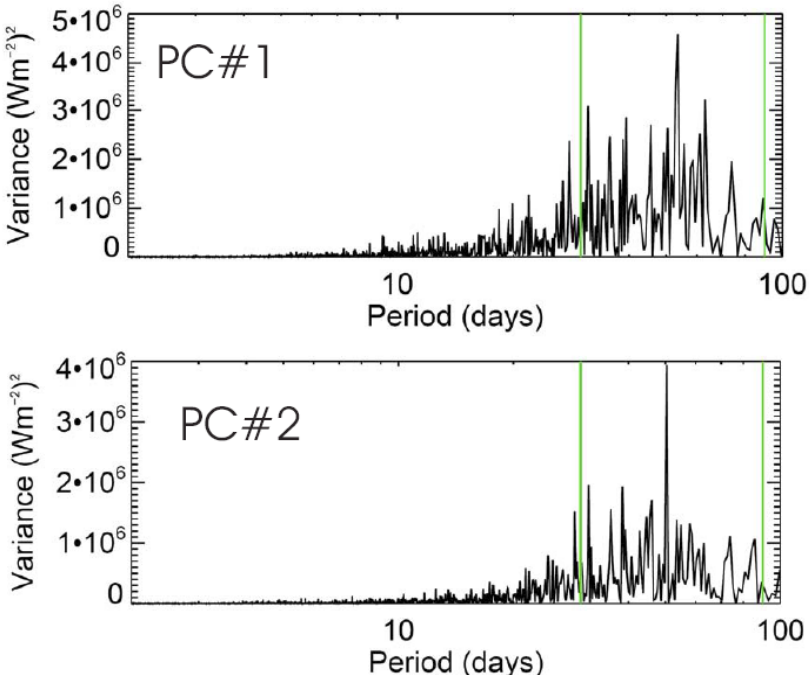

Figure 7. First two EOFs and the Fourier spectra of their corresponding PC's for unfiltered daily anomalies (relative to the annual cycle) of OLR for all the summers (May to September) from 1980 to 2005.

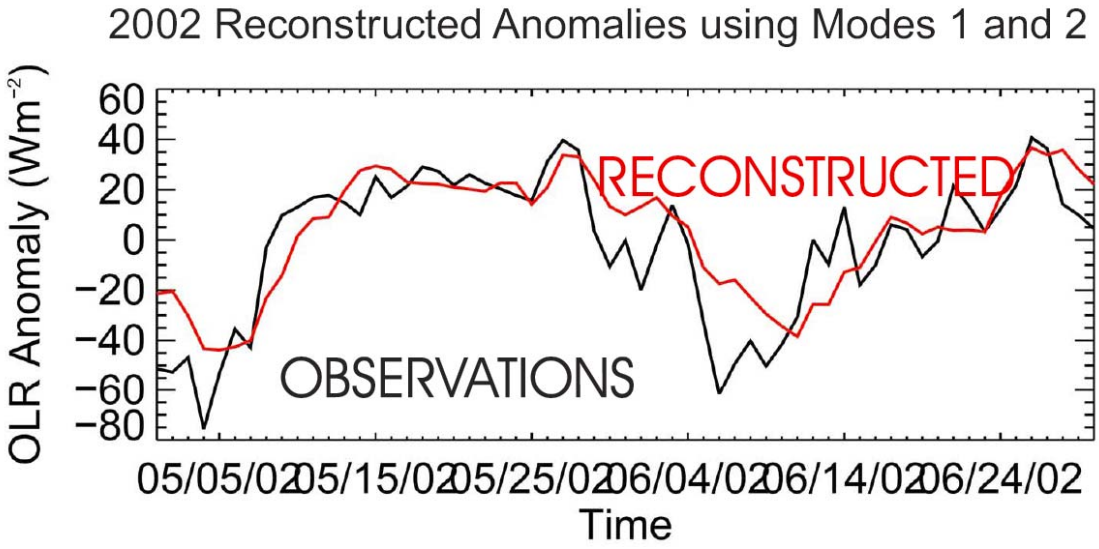

Figure 8. Reconstructed Anomalies of OLR using EOFs 1 and 2 shown in Figure 7.

a) Predictor (Relative Vorticity) and Predictand (OLR)

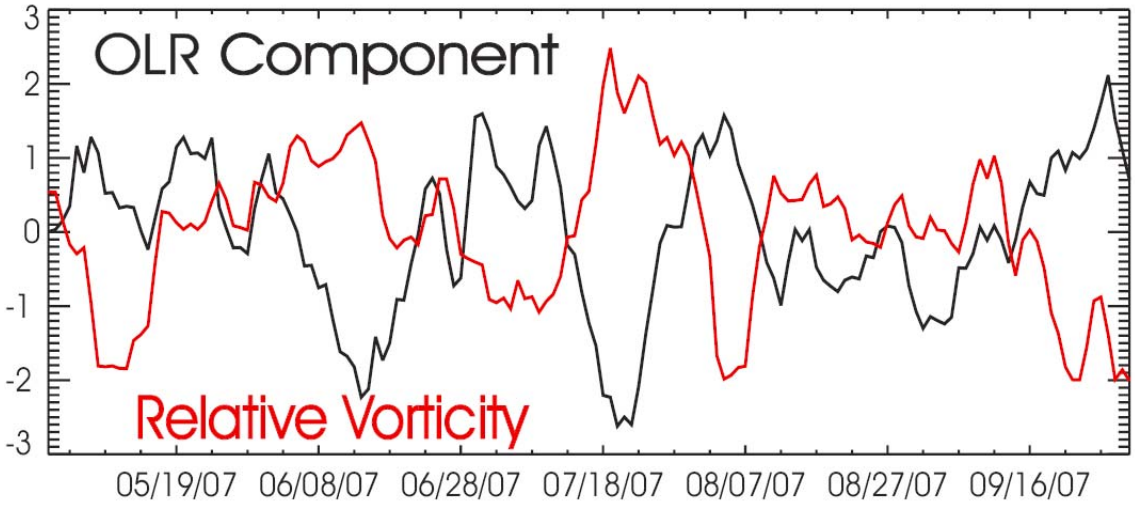

b) Correlations and scatter plot between relative vorticity and OLR.

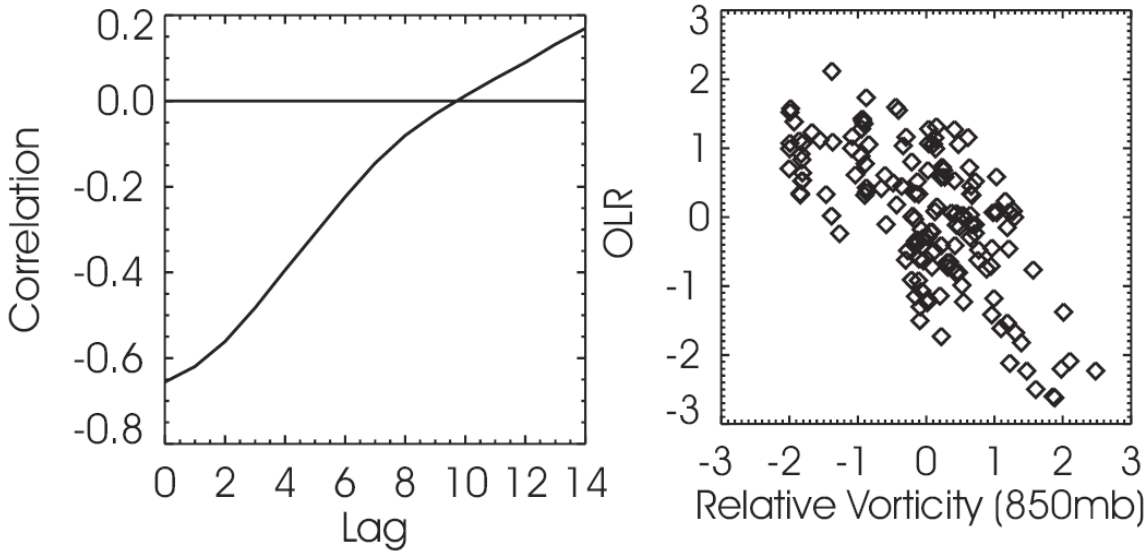

Figure 9. a) Predictor (Relative Vorticity) and Predictand (OLR). b) Correlations and scatter plot between relative vorticity and OLR.

a) Raw ECMWF forecasts projected onto EOF1

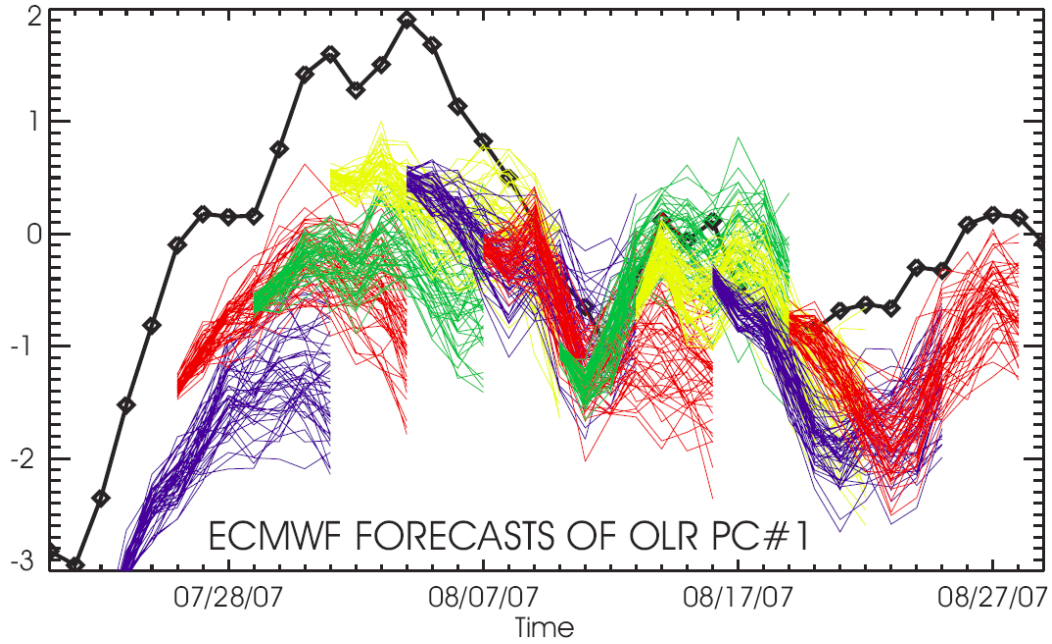

b) Hybrid Forecast of OLR (PC1)

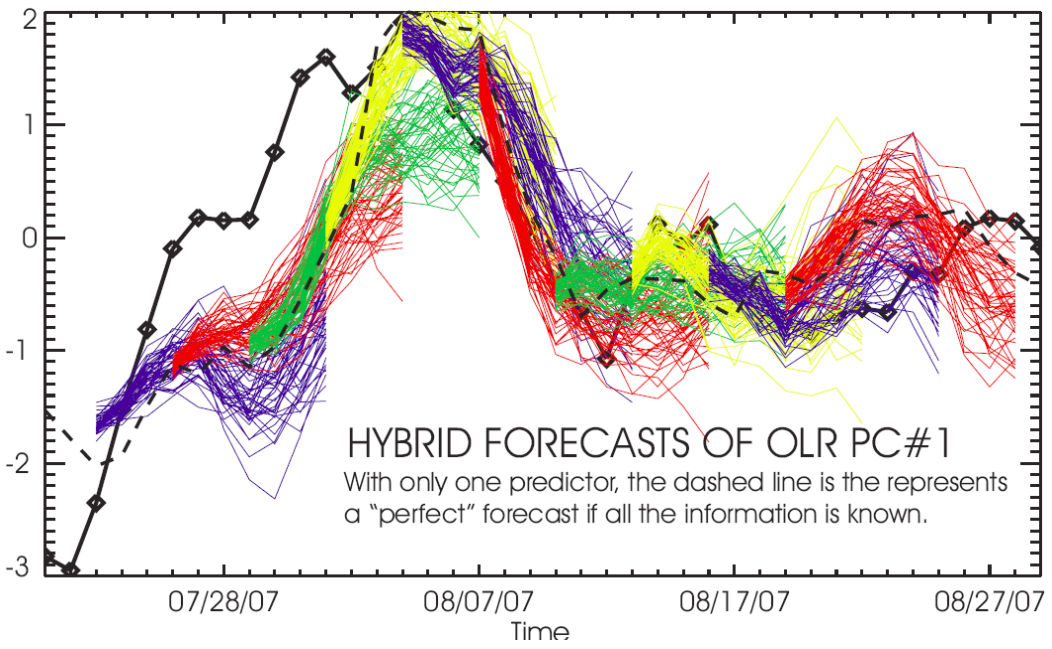

Figure 10. a) Raw ECMWF forecasts projected onto EOF1 and b) Hybrid Forecast of OLR (PC1). The different colors are used to distinguished between forecasts of different dates. The multiple lines for each forecast represent each ensemble member. Te dashed line corresponds to the best possible forecast (e.g. skill potential) as it represents the hybrid OLR hindcast assuming that 850mb vorticity is known.